



Project: **SEAWave**

Maximum macroscopic skin exposure

Work Package: WP5

Deliverable: D5.1

Deliverable No.: D15

Abstract

The upper part of the frequency spectrum (millimeter waves, MMW) applied by modern communications technologies (5G and beyond), makes skin the dominantly exposed tissue to electromagnetic fields. Therefore, an animal study on murine skin carcinogenicity and other endpoints will be implemented within SEAWave project. This deliverable aims to contribute to the dosimetry of the animal study, considering the complex and dynamic anatomy of murine skin, by evaluating the absorbed power at various depths and locations, thus facilitating the correlation between these data with the observed endpoints.

Project Details

Project name	SEAWave
Grant number	101057622
Start Date	01 Jun 2022
Duration	36 months
Scientific coordinator	Prof. Th. Samaras, Aristotle University of Thessaloniki (AUTH)

Deliverable Details

Deliverable related number	D5.1
Deliverable No.	D15
Deliverable name	Maximum macroscopic skin exposure
Work Package number	WP5
Work Package name	Macro and Microdosimetry in the Human and Murine Skin
Editors	S. Iakovidis, Prof. T. Samaras, AUTH
Distribution	Public
Version	1.0
Draft/final	Final
Keywords	Dosimetry, skin exposure, mmWave, animal study

Contents

1	Introduction	4
2	Objective.....	4
3	Materials and Methods	4
3.1	Mouse skin model	4
3.2	Computational method	9
4	Results and Discussion.....	10
5	Conclusions.....	13
6	References	13

1 Introduction

The evolution of mobile communications facing new demands regarding speed (high-data rates), synchronization (low-latency), and the number of connected devices (IoT), has led the industry to use upper part of the frequency spectrum (millimeter waves, MMW). Compared to the well-studied lower part of the frequency spectrum, MMW electromagnetic fields impose new challenges to the study of potential health effects on humans. Their lower wavelength results in significantly lower penetration depth in human tissues [1]. Thus, skin as the outermost tissue of the human body, is dominantly exposed and consequently studied [2]. Skin is an organ with a highly complex anatomy involving different types of cells at different depths. Moreover, it is an organ with a dynamic anatomy, since the distribution of these different types of cells changes with time (e.g., keratinization, hair cycle).

2 Objective

The present deliverable aims to contribute to the dosimetry of the animal study on skin carcinogenicity, which will be performed within the SEAWave Project. The irradiated animals will be mice; therefore, the deliverable focuses on the exposure of murine skin. Taking into account the above, it is necessary to be able to correlate the absorbed power at various depths and locations of cell types with the observed endpoints, since different cell types in the skin give different types of cancer.

3 Materials and Methods

A dosimetric study of the irradiated subjects (mice) of the animal study is initially performed. Ptch1+/- mice (equal numbers from the two sexes) will be whole-body exposed for 23 hours daily to MMW radiation (27.5 GHz) from birth to six months of age (6M). The study is focused on skin since this is the tissue that dominantly absorbs electromagnetic energy at this frequency. A planar stratified model of mice skin layers is considered. An analytical solution of Maxwell's equations for this model is used to evaluate the field values and other relevant dosimetric quantities inside the skin. The aforementioned approach is validated against a commercially available software widely used in such studies (Sim4Life), which implements the Finite-Difference Time-Domain (FDTD) method. Variations emanating from variations of skin layers dimensions and dielectric properties (dielectric constant, conductivity) due to age, are also evaluated.

3.1 Mouse skin model

The mouse skin model developed in this study follows the approach of human skin models already used for dosimetric studies, e.g., [1], [3], [4] and [5]. In this context, a planar geometrical

model is used to model mouse skin and underlying tissues, consisting of five different layers (Figure 1): a) Keratinized stratum (KS), consisting of stratum corneum and stratum lucidum, b) Viable Epidermis (VE), c) Dermis (DE), d) Adipose tissue (fat, FT) and e) Muscle (MS).

These layers can be identified in a H&E (hematoxylin & eosin) stained, cross-sectional mouse skin sample image (Figure 2).

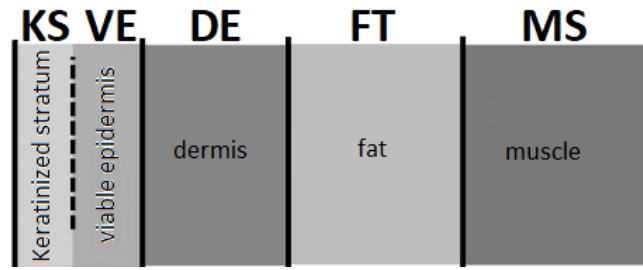


Figure 1. Layered model of mouse skin used for dosimetric study

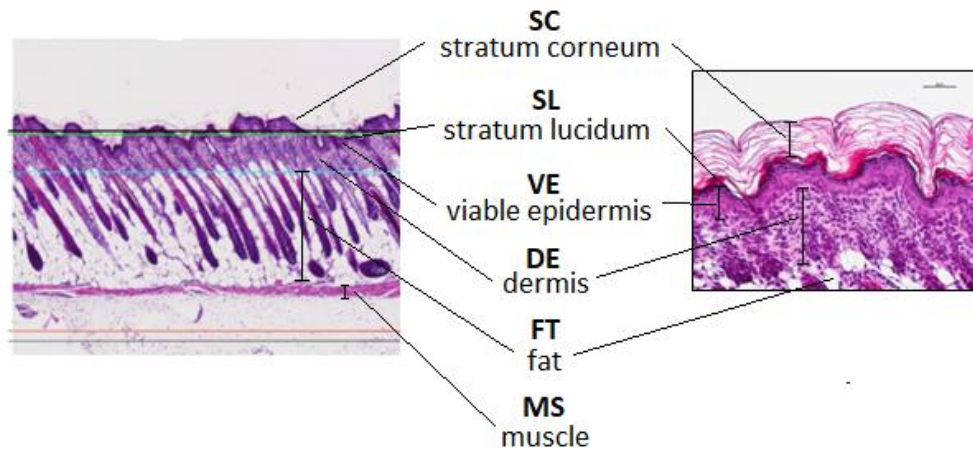


Figure 2. H&E-stained images of cross-sectional mouse skin samples and layer identification

For the determination of the skin layers' thicknesses, mean values are available in the literature [6]. However, large variations with age are observed, especially throughout the hair cycle (Figure 3) [7], [8], [9].

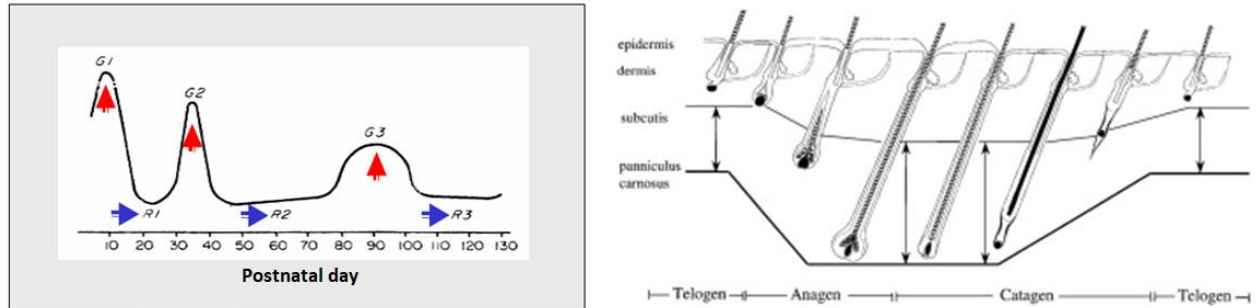


Figure 3. Skin layers' variation during a hair cycle [9]

The hair cycle is a periodic phenomenon that lasts approximately 21 days and occurs many times throughout the life period of a mouse. To capture the variations of skin layers' thicknesses over a hair cycle, the skin layering of three mice was measured at each of five different time instances of the first cycle (postnatal days 2, 5, 10, 15 and 21). Twelve values for each layer thickness among three different individuals were measured for each of the five different postnatal days. The measurements were performed on haematoxylin and eosin (H&E) stained skin samples. Images were captured using a Nikon Eclipse E800 microscope and analyzed by NIS-Elements BR 5.3. The measurement results are summarized in Table 1.

Table 1. Measurements of mouse skin layers' thicknesses during the first hair cycle

Postnatal Day	Layer thickness (μm)	Keratinized stratum	Viable Epidermis	Dermis	Hypodermis	Muscle	Total
P2	mean	69.39	21.57	94.62	134.16	49.11	368.84
	std	5.57	5.10	41.94	49.28	12.46	
P5	mean	45.83	37.91	132.43	514.88	38.51	769.55
	std	6.79	8.86	26.16	81.35	19.12	
P10	mean	50.37	23.16	169.34	644.14	42.39	929.40
	std	6.57	4.68	12.42	68.64	8.21	
P15	mean	16.14	18.46	149.49	597.14	19.21	800.93
	std	2.84	4.69	20.42	45.08	2.49	
P21	mean	14.45	16.33	183.14	63.59	50.05	327.57
	std	3.35	3.94	43.63	31.30	24.73	

Due to lacking information on the dielectric properties of the different mouse skin layers considered here, the corresponding ones for human skin were used. This approach is largely used in the literature since the availability of data about specific species is limited and the variations of tissue dielectric properties within a species may well exceed variations between species, as suggested in [10].

The dielectric properties of human skin layers were determined following the approach suggested in [1] and used also in [3] and [11]. The one-term Debye model [1] was used to calculate the properties for the considered frequency (27.5 GHz). The applied values are summarized in Table 2.

Table 2. Dielectric properties assumed for mouse skin at 27.5 GHz

Skin Layer	Relative Permittivity	Conductivity (S/m)
KS (Keratinized Stratum)	3.58	1.13
VE (Viable Epidermis)	17.38	25.81
DE (Dermis)	17.38	25.81
FT (Fat)	3.54	2.19
MS (Muscle)	23.53	37.42

It is worth mentioning that the values reported in Table 2 correspond to adult individuals. However, it is known that these properties vary with age [4], [12], [13]. In the gigahertz frequency range, electromagnetic fields interaction with tissues dominantly results from free water molecule polarization (γ dispersion) [5]. The water content of tissues varies with age and so do the dielectric properties. In this context, the Total Body Water (TBW), defined as the ratio of the mass of the water in an individual's body to the total mass of the body, is used as a proxy for the evaluation of variations of the dielectric properties with age [4], [13]. Wang *et al* [13] applied Lichtnecker's logarithmic formula (1), considering tissues as a mixture of organic material and water.

$$\varepsilon_r = \varepsilon_{rw}^\alpha \cdot \varepsilon_{rt}^{1-\alpha} \quad (1)$$

where ε_{rw} is the relative permittivity of water, ε_{rt} is the relative permittivity of the organic material and α is the hydration rate ($\alpha = \rho \cdot \text{TBW}$, where ρ is the mass density). Since the relative complex permittivity of a tissue $\dot{\varepsilon}_r$ is given by

$$\dot{\varepsilon}_r = \varepsilon_r' - j\varepsilon_r'' = \varepsilon_r - j \frac{\sigma}{\omega \varepsilon_0} = \varepsilon_r \left(1 - j \frac{1}{\omega \tau} \right) \quad (2)$$

where $\tau = \frac{\varepsilon_r \varepsilon_0}{\sigma}$. Substituting (2) into (1) results in

$$\dot{\varepsilon}_r = \varepsilon_{rw}^{\frac{\alpha - \alpha_A}{1 - \alpha_A}} \cdot \varepsilon_{rA}^{\frac{1 - \alpha}{1 - \alpha_A}} \left(1 - j \frac{1}{\omega \tau} \right) \quad (3)$$

where ε_{rA} is the relative permittivity for adult tissue and α_A is the hydration rate for adult tissue. Equation (3) gives the complex permittivity at different ages if the TBW as a function of age is known and the dielectric properties at adulthood are also known. This approach was followed by Sacco *et al* [4] to evaluate the age-dependence of electromagnetic power deposition in human

skin. The authors considered no variations of TBW on the outermost skin layer (i.e., SC) with age, since this layer is mostly impacted by environmental and physiological conditions.

Following the approach of Wang [13] and Sacco [4] and considering that the dielectric properties of the skin layers at adulthood are known (Table 2), it was necessary to determine the TBW of mice as a function of age in the literature. In [14], Bailey *et al* studied the body composition of 111 white male mice in terms of protein, water, fat and ash as a function of age. Data for only 16 of them are published (Figure 4). Curve fitting of these data, using the least square method, results in

$$TBW = -2.93 \cdot \ln(\text{age}) + 79.97 \quad (4)$$

where TBW is evaluated in terms of percentage and age in terms of postnatal days. The relative permittivity of water was evaluated using the Ellison *et al* model [15], for a temperature of 32.6 °C [5], while the mass density values applied for each skin layer were those given in [4]. The variations of dielectric properties as a function of age (postnatal days) for the considered skin layers are plotted in Figure 5. Significant variations are present during the first days of life, following the corresponding variations of TBW. The dielectric properties tend to a constant value after few tenths of postnatal days.

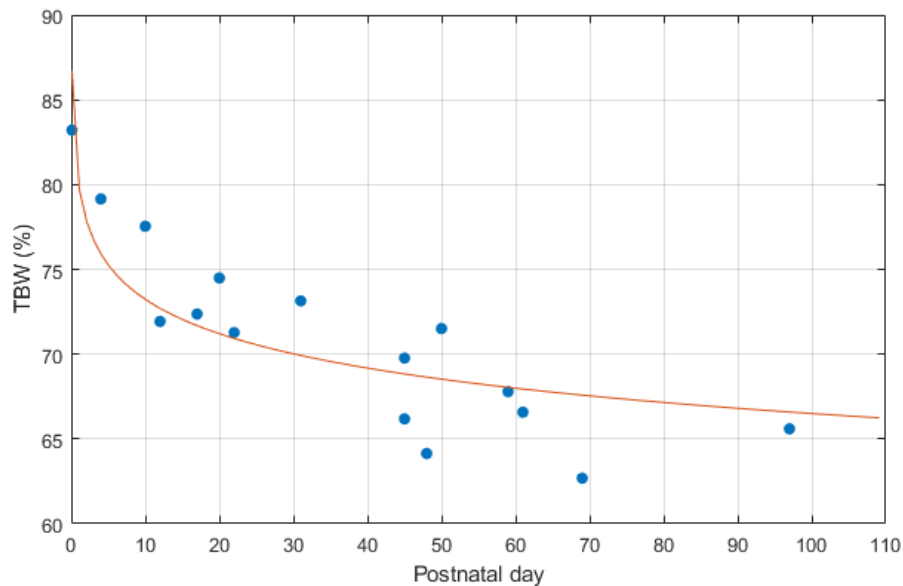


Figure 4. TBW of 16 mice vs age [14] and fitting curve

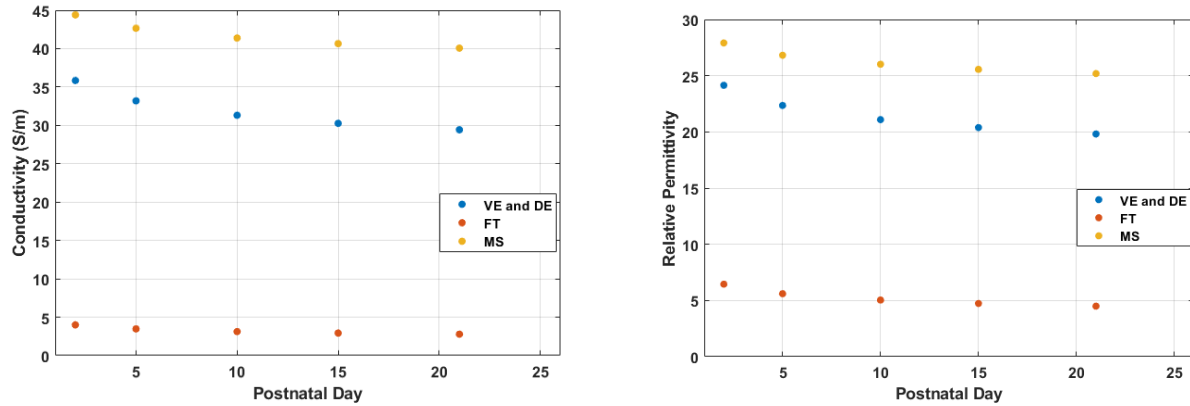


Figure 5. Conductivity (left) and relative permittivity (right) vs age for mouse skin layers (Viable Epidermis, Dermis, Fat and Muscle)

3.2 Computational method

The stratified mouse skin model presented in §3.1 (Figure 1) was used for the electromagnetic analysis.

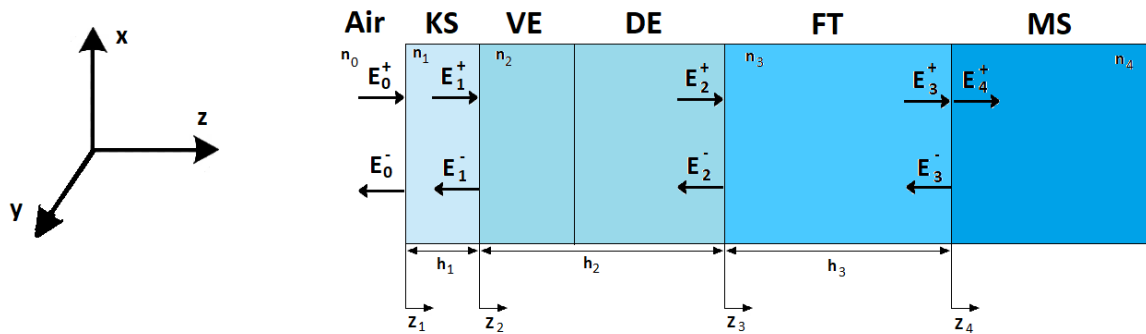


Figure 6. Stratified mouse skin model used for electromagnetic analysis

The model considered here is irradiated with a TEM-polarized plane wave. The direction of the propagation (along z-axis) is perpendicular to the interfaces of the skin layers (Figure 6). The electric (E) and magnetic (H) field values are calculated analytically using the transmission and reflection coefficients at all tissue interfaces [16]. The muscle layer is considered as the terminating layer, i.e., no reflections at the tissue interfaces underlying the muscle layer are taken into account. This approach has already been applied successfully in previous studies [3], [4], [11] and offers an important speed advantage over other computational methods (e.g., FDTD, FEM). The calculation was performed with MATLAB (The MathWorks Inc., Natick, MA, USA). The developed MATLAB code was verified against a commercially available software (Sim4Life, ZMT, Switzerland) which implements the FDTD method (Figure 7).

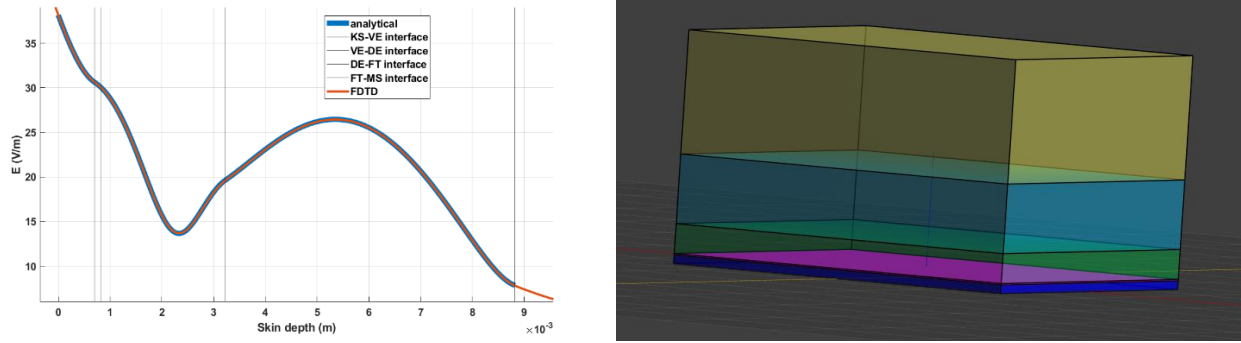


Figure 7. Model validation: E field values comparison (left), stratified model used with FDTD method (right): Muscle (yellow), Fat (cyan), Dermis (green), Viable epidermis (pink), Keratinized stratum (blue)

A stratified model of skin was also used with the FDTD method (Figure 7, right). Periodic boundary conditions were used on the sides and perfectly matched layers on top and bottom. The model was irradiated with a TEM plane wave of incident power density of 1 W/m^2 in air. As can be inferred from Figure 7 (left), the results using the two methods are in a very good agreement (deviation $< 0.4 \%$).

According to the International Commission on Non-Ionizing Radiation Protection (ICNIRP), the absorbed power density (APD) level, S_{ab} (W/m^2), is considered the relevant metric for the basic restriction for frequencies higher than 6 GHz [17]. Consequently, S_{ab} is evaluated at the interfaces of the skin layers by using the formula based on the Poynting vector \mathbf{S} :

$$S_{ab} = \iint_A \text{Re}[\mathbf{S}] \cdot \frac{d\mathbf{s}}{A} = \iint_A \text{Re}[\mathbf{E} \times \mathbf{H}^*] \cdot \frac{d\mathbf{s}}{A} \quad (5)$$

The mean value of absorbed power density within each skin layer, $\overline{S_{ab}}$, is also evaluated:

$$\overline{S_{ab}} = \frac{\int_{z_1}^{z_2} S_{ab}(z) dz}{\int_{z_1}^{z_2} dz} \quad (6)$$

where z_1, z_2 are the coordinates of the limits of the considered layer. The power loss per normal surface area within each layer of the skin is then calculated by the difference of the power density entering the layer minus the power leaving it:

$$PL = S_{ab}(z_2) - S_{ab}(z_1) \quad (7)$$

4 Results and Discussion

The dosimetric study of mouse skin is focused on the first hair cycle (postnatal days 2-21). The reason for the selection of this time period of mouse life is twofold: a) The largest variability of mouse skin thickness occurs during this period (Figure 3). b) The largest variability of the dielectric properties of mouse skin layers also occurs during this period (Figures 4 and 5). Consequently,

the absorbed power density and the power loss, are expected to vary more during this time period compared to any other. As a result, the study of this time period provides the safest way to evaluate the worst-case scenario.

The variability of the skin layers' thickness during the first hair cycle is presented in Figure 8. Thickness values correspond to four different evaluation points for each of the three different individuals measured at five different postnatal days. Thus, the variability presented in Figure 8 originates from sampling uncertainty (four different evaluation points) and interindividual variability (three different mice), which also includes sex variability, since the three mice are of both sexes. However, the small sample size imposes problems to the statistical analysis based on these parameters. The significant variation of the skin thickness throughout a hair cycle, dominated by the variation of the subcutaneous fat layer, presented in Figure 3, is confirmed by the measurement results shown in Figure 8.

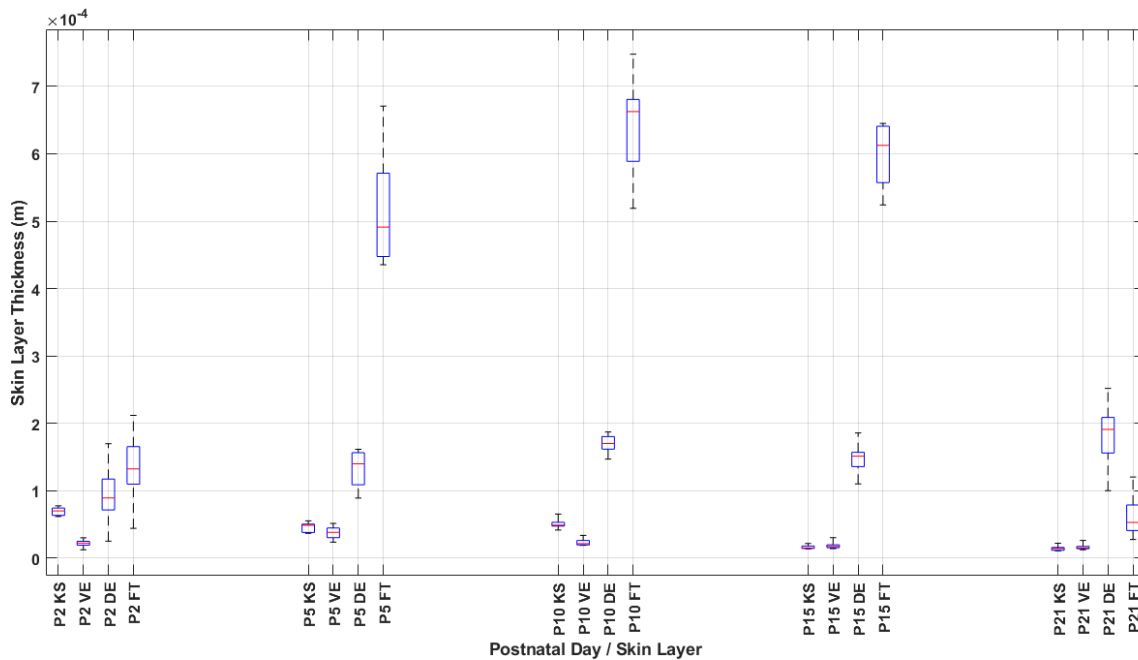


Figure 8. Skin layers' thickness at different postnatal days (2-21): median (red line), interquartile range (blue box) and min-max values (dotted black line). KS: Keratinized Stratum, VE: Viable Epidermis, DE: Dermis, FT: Fat, MS: Muscle

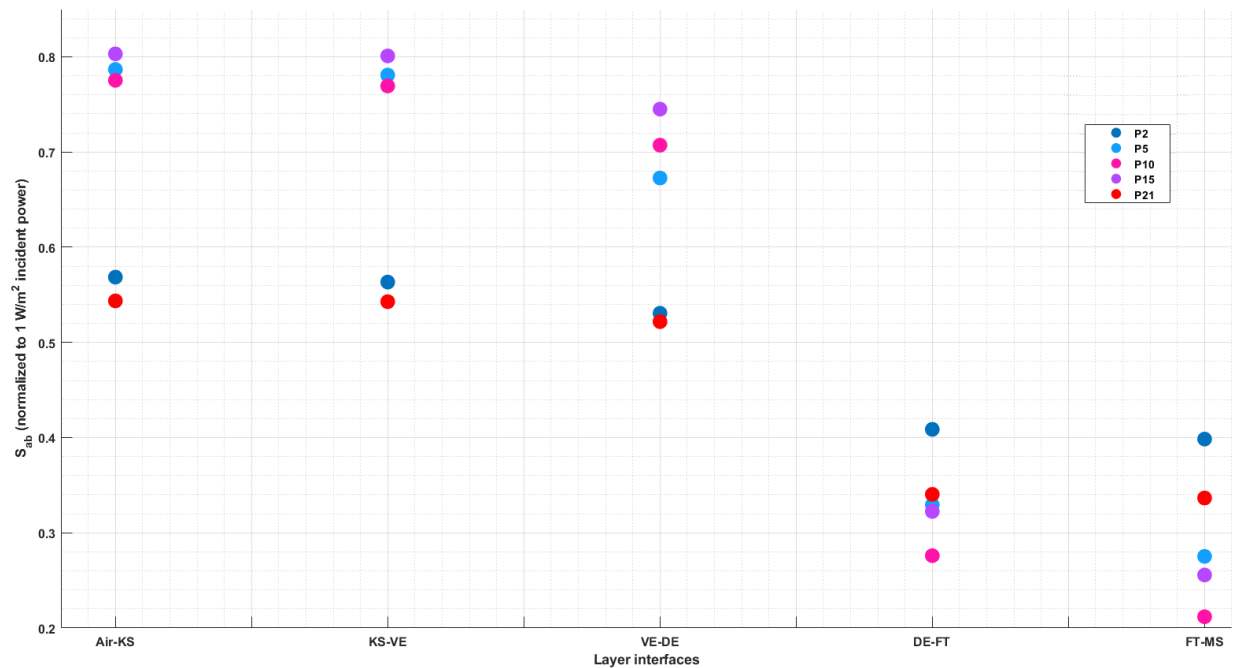


Figure 9. APD, S_{ab} , at skin layer interfaces for different postnatal days

Applying the mean values for layer thicknesses at different postnatal days and the dielectric properties for adult subjects, the absorbed power density at layer interfaces is evaluated (Figure 9). Large variations of S_{ab} during the first hair cycle are observed that are attributed to the large corresponding variations of skin layers' thickness (Figure 8).

In Figure 10 the distribution of power loss at each of the skin layers (KS, VE, DE and FT) is presented using boxplot charts: The median value (red line), interquartile range (blue box) and max/min values (dotted black line) of the distribution, corresponding to the distribution of skin layers thickness measurements (Figure 8), are plotted. The same distribution considering the dielectric properties variations with age, is also plotted and indicated by "TBW" in the same figure for comparison. The comparison shows that the impact of considering dielectric variations with age is significant, yet much lower than the impact of skin layers thickness variation on the power loss within each skin layer. The maximum power per normal surface area deposited within any skin layer and for any postnatal day is 0.42 W/m^2 (fat layer on postnatal day 15).

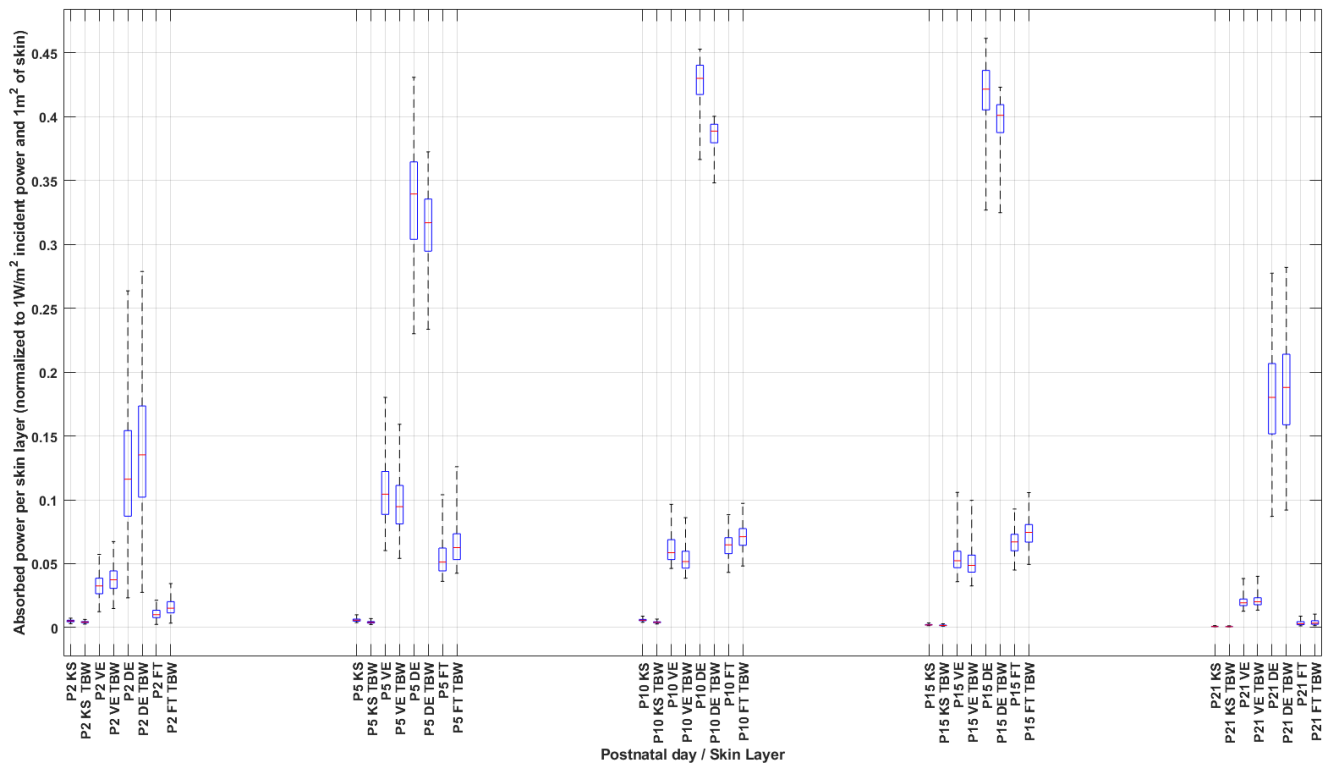


Figure 10. Power loss at each skin layer (KS, VE, DE, FT), at different postnatal days (P2, P5, P10, P15, P21), when considering the variation of dielectric properties with TBW (denoted with 'TBW' at the end) or not

5 Conclusions

A dosimetric study for mouse skin irradiated at 27.5 GHz and normal incidence was performed. The results of this study will initially be used for defining the exposure levels in the animal study and, later, for assessing the risk for cancer initiation or promotion in the mice. The study was performed at the macroscopic scale, taking into account (for the first time) the variation of skin layers' thicknesses due to the hair cycle and the changes in the dielectric properties due to age. It was shown that the impact of layer thickness variation on dosimetric metrics is significantly larger compared to the one of dielectric properties due to age. The full dosimetric evaluation of murine skin needs to consider the layer of fur, as well as the appendages in the skin, i.e., the microscopic scale in which work is ongoing.

6 References

- [1] M. C. Ziskin, S. I. Alekseev, K. R. Foster, and Q. Balzano, "Tissue models for RF exposure evaluation at frequencies above 6 GHz", *Bioelectromagnetics*, vol. 39, no. 3, pp. 173-189, doi: 10.1002/bem.22110, 2018

-
- [2] T. Wu, T. S. Rappaport, and C. M. Collins, "Safe for Generations to Come: Considerations of Safety for Millimeter Waves in Wireless Communications", *IEEE Microwave Magazine*, vol. 16, no. 2, pp. 65-84, 2015, doi: 10.1109/MMM.2014.2377587
- [3] A. Christ, T. Samaras, E. Neufeld, and N. Kuster, "RF-Induced Temperature Increase in a Stratified Model of the Skin for Plane-wave Exposure at 6–100 GHz", *Radiation Protection Dosimetry*, vol. 188, no. 3, pp. 350-360, 2020, doi: 10.1093/rpd/ncz293
- [4] G. Sacco, S. Pisa, and M. Zhadobov, "Age-dependence of electromagnetic power and heat deposition in near-surface tissues in emerging 5G bands", *Scientific Reports*, vol. 11, no. 3983, 2021, doi: 10.1038/s41598-021-82458
- [5] S. Alekseev and M. Ziskin, "Human skin permittivity determined by millimeter wave reflection measurements", *Bioelectromagnetics*, vol. 28, no. 5, pp. 331-339, 2007, doi: 10.1002/bem.20308
- [6] N. A. Monteiro-Riviere, D. G. Bristol, T. O. Manning, R. A. Rogers, and J. E. Riviere, "Interspecies and interregional analysis of the comparative histologic thickness and laser Doppler blood flow measurements at five cutaneous sites in nine species", *The Journal of Investigative Dermatology*, vol. 95, no. 5, pp.582-586, 1990, doi: 10.1111/1523-1747.ep12505567
- [7] B. C. Herman, W. Montagna, and J.M. Malone, "Changes in the skin in relation to the hair growth cycle", *The Anatomical Record*, vol. 116, no. 1, pp. 75-81, 1953, doi: 10.1002/ar.1091160107
- [8] L. S. Hansen, J. E. Coggle, J. Wells, and M. W. Charles, "The influence of the hair cycle on the thickness of mouse skin", *The Anatomical Record*, vol. 210, no. 4, pp. 569-573, 1984, doi: 10.1002/ar.1092100404.
- [9] S. Müller-Röver, B. Handjiski, C. van der Veen, S. Eichmüller, K. Foitzik, I. A. McKay, K. S. Stenn, and R. Paus, "A Comprehensive Guide for the Accurate Classification of Murine Hair Follicles in Distinct Hair Cycle Stages", *The Journal of Investigative Dermatology*, vol. 117, no. 1, pp. 3-15, 2001, doi: 10.1046/j.0022-202x.2001.01377.x
- [10] P. Weddle, T. Vincent, R. J. Kee, S. Gauthier, S. I. Abarzhi, K. R. Sreenivasan -, S. Gabriel, R. W. Lau, and C. Gabriel, "The dielectric properties of biological tissues: II. Measurements in the frequency range 10 Hz to 20 GHz", *Physics in Medicine & Biology*, vol. 41, no. 11, pp. 2251-2269, 1996, doi: 10.1088/0031-9155/41/11/002
- [11] A. Christ, T. Samaras, E. Neufeld, and N. Kuster, "Transmission coefficient of power density into skin between 6 and 300 GHz", *Radiation Protection Dosimetry*, vol. 192, no. 1, pp. 113-118, 2020, doi: 10.1093/rpd/ncaa179

-
- [12] A. Peyman, A. A. Rezazadeh, and C. Gabriel, "Changes in the dielectric properties of rat tissue as a function of age at microwave frequencies", *Physics in Medicine & Biology*, vol. 46, no. 6, pp. 1617-1629, 2001, doi: 10.1088/0031-9155/46/6/303
- [13] J. Wang, O. Fujiwara, and S. Watanabe, "Approximation of aging effect on dielectric tissue properties for SAR assessment of mobile telephones", *IEEE Transactions on Electromagnetic Compatibility*, vol. 48, no. 2, pp. 408-413, 2006, doi: 10.1109/TEMC.2006.874085
- [14] C. B. Bailey, W. D. Kitts, and A. J. Wood, "Changes in the gross chemical composition of the mouse during growth in relation to the assessment of physiological age", *Canadian Journal of Animal Science*, vol. 40, no. 2, pp. 143-155, 1960, doi: 10.4141/cjas60-022
- [15] W. J. Ellison, "Permittivity of pure water, at standard atmospheric pressure, over the frequency range 0-25 THz and the temperature range 0-100 °C", *Journal of Physical and Chemical Reference Data*, vol. 36, pp. 1-18, 2007, doi: 10.1063/1.2360986
- [16] S. J. Orfanidis and T. Monica, 2016 (Aug 1). *Electromagnetic Waves and Antennas* [Online]. Available: <https://www.ece.rutgers.edu/~orfanidi/ewa/>
- [17] International Commission on Non-Ionizing Radiation Protection (ICNIRP), "Guidelines for limiting exposure to electromagnetic fields (100 kHz to 300 GHz)", *Health Physics*, vol. 118, no. 5, pp. 483-524, 2020, doi: 10.1097/HP.0000000000001210